Published in final edited form as:
Brain Res. 2009 December 15; 1303: 179–194. doi:10.1016/j.brainres.2009.09.063.

Insulin and IGF-I prevent brain atrophy and DNA loss in diabetes

Predrag Šerbedžija[a], **James E. Madl**[b], and **Douglas N. Ishii**[a,b]

[a]Department of Biochemistry and Molecular Biology, Colorado State University, Fort Collins, CO 80523, USA

[b]Department of Biomedical Sciences, Colorado State University, Fort Collins, CO 80523, USA

Abstract

The aim of this study was to identify factors that regulate the bulk of adult brain mass, and test the hypothesis that concomitantly reduced insulin and insulin-like growth factor (IGF) levels are pathogenic for brain atrophy associated with impaired learning and memory in diabetes. Doses of insulin, or insulin plus IGF-I that were too small to prevent hyperglycemia were infused for 12 weeks into the brain lateral ventricles of streptozotocin-diabetic adult rats. Brain wet, water and dry weights were significantly decreased in diabetic rats; insulin prevented these decreases. The decrease in brain DNA and protein contents in diabetic rats was prevented by the combination treatment, but not by insulin alone. Levels of several glia- and neuron-associated proteins were reduced in diabetes; these reductions were also prevented by the combination treatment. Although hyperglycemia was not prevented in plasma nor cerebrospinal fluid, insulin prevented brain atrophy but not bulk DNA loss in diabetes, whereas the combination prevented both. Insulin actively prevented the loss of brain water content as well. Brain atrophy is associated with concomitantly reduced levels of insulin and IGF in other disorders such as Alzheimer's disease.

Keywords

Dementia; Insulin-like growth factor; Encephalopathy; Neurodegeneration; Brain edema; Diabetic neuropathy

1. Introduction

Diabetes increases the risk for brain atrophy, dementia, and late-onset Alzheimer's disease. Brain atrophy contributes to dementia, and factors regulating adult brain mass need to be identified. We tested whether treatments with insulin and IGF are able to ameliorate or prevent brain atrophy in STZ-treated rats.

Brain atrophy in type 1 diabetes (Araki et al., 1994; Perros et al., 1997) is not correlated with hypoglycemic episodes (Lunetta et al., 1994), and may contribute to cognitive impairments, including learning and memory deficits (Fox et al., 2003; Prescott et al., 1990; Ryan et al., 1993). Type 2 diabetic patients without cerebrovascular disease also have increased risk for brain atrophy (Araki et al., 1994; den Heijer et al., 2003) and dementia (Cukierman et al.,

Correspondence: Dr. D.N. Ishii, Department of Biomedical Sciences, Colorado State University, Fort Collins, CO 80523, USA. Telephone or Fax: +1 970 491 7339. Douglas.Ishii@ColoState.edu.

2005; Ott et al., 1999), showing that diabetes poses a risk factor separate from microvascular disease. Brain lesions (Araki et al., 1994; Dejgaard et al., 1991), degeneration of neurons, and axonal loss (Reske-Nielsen and Lundbaek, 1963) are observed post-mortem. Contributing factors may include increased glucose and polyol levels, protein glycation, cerebrovascular disease, oxidative stress, and/or reduced growth factor levels.

Substantial evidence shows that diabetic patients have diminished brain insulin and IGF (see Abbreviations) signaling. Brain insulin is primarily derived from the circulation by transport across the blood-brain-barrier (Woods et al., 2003). Insulin levels are reduced in type 1 diabetes, while resistance to insulin is coupled with a partial reduction of insulin production in type 2 diabetes. IGF gene expression is reduced in STZ-diabetic rat brain (Wuarin et al., 1996) and liver, the primary source of circulating IGF. Serum and brain IGF-I levels are reduced (Busiguina et al., 2000; Olchovsky et al., 1990). Circulating IGF levels decline with both aging and diabetes in humans (Tan and Baxter, 1986). IGF-I crosses the blood-brain-barrier (Pulford and Ishii, 2001) and supports learning and memory (Lupien et al., 2003); human cognitive performance correlates with serum IGF-I levels (Rollero et al., 1998).

Conditional knock-out of the brain neuronal IR gene has no detectable effect on brain weight, morphology (Bruning et al., 2000), brain glucose utilization, nor learning and memory (Schubert et al., 2004). However, because insulin and IGF provide cooperative neurotrophic support (Recio-Pinto and Ishii, 1984; Wang et al., 1992), IGF might compensate for such knockout.

A concomitant decline in signaling through the insulin and IGF systems may increase risk for brain atrophy and degeneration in diabetes (Fig. 1). The following hypotheses were tested: i) Insulin prevents the loss of adult brain mass through predominantly non-glucoregulatory processes in diabetes, ii) Insulin regulates brain water content, and iii) Insulin with IGF provide greater protection against brain atrophy and degeneration than insulin alone. Because total brain mRNA and protein levels are reduced (Lupien et al., 2006) and a catabolic state may contribute to the loss of brain mass, we further tested whether insulin and IGF can prevent brain atrophy by preventing loss of total protein and cell-type specific proteins.

2. Results

The theoretical basis for this study is set forth in Fig. 1. Concomitantly reduced insulin and IGF levels are required to test the hypothesis, and this occurs in the STZ-diabetic rat (Lupien et al., 2006). If insulin were administered peripherally in diabetes, hyperglycemia would be reduced via Path A while growth factor activity would be simultaneously increased via Path B; uncertainty would remain as to which path contributed to brain atrophy. Consequently, in order to test the previously stated hypotheses, Path A hyperglycemia was held constant by infusing into the brain lateral ventricles doses of either insulin or its combination with IGF-I that were far too small to prevent hyperglycemia. To prevent hyperglycemia in STZ-diabetic rats, 9.5 IU insulin/kg/day s.c. is required (Wuarin et al., 1996), whereas this study infused insulin i.c.v. at only 3.3% of that dose rate. Treatments were initiated at the time of induction of diabetes, and both duration of diabetes and treatments were for 12 weeks.

2.1. Insulin and the combination treatment prevented loss of brain wet, water, and dry weights in diabetic rats

Note that statistical data associated with figures are summarized in Table 1 in the order data are presented. Atrophy involved loss of brain mass and water after 12 weeks of diabetes. Brain wet weight was significantly lower in D+aCSF *vs.* Non-D rats (Fig. 2A-C).

An aliquot of brain homogenate was lyophilized, and water and dry weights were significantly lower in D+aCSF *vs.* Non-D rats. Brain water weight comprised 79%, whereas dry weight comprised 21% of total wet weight in Non-D rats. There was a significant 9-10% loss of brain wet, water, and dry weights in D+aCSF rats.

Insulin treatment completely prevented the loss of brain wet, water, and dry weights in D+Ins *vs.* D+aCSF rats. Values for D+Ins were no longer significantly different from Non-D with respect to wet, water or dry weights. The combination treatment also prevented the loss in brain wet, water, and dry weights *vs.* D+aCSF rats, and treatment was superior to insulin alone, because the brain wet, water and dry weights were greater *vs.* D+Ins rats. Brain dry weight was significantly higher in D+Ins+IGF *vs.* Non-D rat brains, and greater brain wet weight was virtually significant.

2.2. The combination, but not insulin alone, prevented the loss of DNA and protein contents per brain in diabetic rats

Other brain samples from the same rats were processed to measure DNA and protein levels, and these data showed that brain atrophy included degeneration with cell loss. There was a significant decrease in bulk DNA and protein contents per brain in D+aCSF *vs.* Non-D rats (Fig. 2D, E). Non-D rats had 248 mg protein per brain (57% of dry weight), consistent with expectation. Protein content per brain trended higher, but was not significantly different in D +Ins *vs.* D+aCSF rats. Insulin alone had no detectable effect on the loss of bulk brain DNA content in diabetic rats; this result does not exclude the possibility that insulin may prevent the loss of cells in limited brain regions.

The combination treatment prevented the loss of both DNA and protein *vs.* D+aCSF rats. It was more effective than insulin alone, for it resulted in a larger DNA content per brain *vs.* D +Ins rats. The combination treatment, moreover, increased DNA content per brain *vs.* Non-D rats.

2.3. The combination, but not insulin alone, prevented the loss of ubiquitous actin, α-tubulin and β-tubulin proteins per brain in diabetic rats

Western blots of total brain proteins may reveal how specific proteins that are expressed in relatively high abundance may contribute to the loss of total protein. Actins and tubulins are major ubiquitous proteins that contribute significantly to bulk brain protein content, and their levels are potentially reduced in diabetes. Actins are often used to normalize Western blots, but actin levels may not be invariant in diabetes. MAB1501 recognizes a highly conserved region of actin, and this pan-actin antibody binds to all six isoforms of vertebrate actin. Western blots detected only a single band of ~43 kDa in brain supernatants from Non-D rats (Fig. 3A). There was a significant reduction in relative actin levels per brain in D+aCSF and D+Ins *vs.* Non-D rats. It seemed that the combination treatment ameliorated such reduction, because there was a trend but not significance between D+Ins+IGF *vs.* D+aCSF rats. There was no significant difference between D+Ins+IGF *vs.* Non-D rats. Insulin alone had no detectable effect.

Antibody clone DM1A detected all four isoforms of α-tubulin as a single band of approximately 53 kDa size in brain supernatants from Non-D rats (Fig. 3B). There was a significant decrease in relative levels of α-tubulins per brain in D+aCSF and D+Ins *vs.* Non-D rats. This decrease was prevented in D+Ins+IGF, but not D+Ins *vs.* D+aCSF rats.

Western blots using clone AA2 detected all 5 isoforms of β-tubulins as a single band of approximately 53 kDa size in brain supernatants from Non-D rats (Fig. 3C). There was a significant decline in relative β-tubulins per brain in D+aCSF and D+Ins *vs.* Non-D rats. This decline was prevented in D+Ins+IGF but not D+Ins *vs.* D+aCSF rats.

2.4. Insulin and the combination treatment prevented the loss of glia-specific proteins GFAP, MBP and PLP per brain in diabetic rats, but glutamine synthetase levels were relatively unchanged

The possibility that there was selective loss of proteins from specific cell types was tested. Selective loss of glia-specific proteins is addressed in this section.

A Western blot specificity study detected bands of appropriate size and immunoreactivity consistent with astrocyte-associated GFAP only in brain and spinal cord, but not liver, intestine, heart, nor kidney supernatants (Supplemental Fig 1 A). A minor band of approximately 45 kDa is believed to be a proteolytic fragment and comprised only 2.3% of the total signal, hence only the 50 kDa band was quantified. Relative levels of GFAP per brain were significantly reduced in D+aCSF *vs.* Non-D rats (Fig. 4A). Insulin as well as the combination treatment prevented this loss *vs.* D+aCSF rats. The latter normalized levels, for there was no difference between D +Ins+IGF *vs.* Non-D rats.

Glutamine synthetase is present in both astrocytes and oligodendrocytes and is comprised of eight identical 45 kDa subunits. Glutamine synthetase is known to be expressed in several tissues, and Western blots showed an expected band at ~42 kDa in supernatants from brain, spinal cord, liver, and kidney, but not heart nor intestine (Supplemental Fig 1B). Relative glutamine synthetase levels were lower but not significantly so in D+aCSF *vs.* Non-D rat brains (Fig. 4B). Insulin and the combination treatment both significantly increased glutamine synthetase levels *vs.* D+aCSF.

Disturbances in oligodendrocyte myelin have been reported in diabetes (see Discussion). PLP is also known as lipophilin. Its extracellular domains are believed to help hold layers of myelin together. Western blots detected a band of ~25 kDa and immunoreactivity consistent with PLP only in brain and spinal cord (Supplemental Fig 1C). Fig. 4C shows a significant reduction in relative PLP levels per brain in D+aCSF *vs.* Non-D rats. Such reduction was prevented in D +Ins+IGF and in D+Ins *vs.* D+aCSF rats. The combination treatment was significantly more effective than D+Ins and increased relative PLP levels above Non-D values.

MBP is also selectively expressed by oligodendrocytes. Due to alternative splicing of a single gene product, transcripts encode four major isoforms. Western blot bands consistent with MBP isoforms were shared in brain and spinal cord samples, but not liver, intestine, heart nor kidney supernatants (Supplemental Fig 1D). The effect of diabetes was studied on the sum of the four isoforms. Fig. 4D shows a significant reduction in relative total MBP levels per brain in D +aCSF *vs.* Non-D rats. Such reduction was prevented in D+Ins *vs.* D+aCSF rats. The combination treatment also prevented this reduction and normalized levels *vs.* Non-D rats.

2.5. The combination, but not insulin alone prevented the loss of the neuron-specific β-tubulin class III, NF-L and NF-M proteins

Having found that there is loss of certain glia-specific proteins in diabetes, we next tested whether there was loss of neuron-specific proteins as well. A single β-tubulin class III band of ~52 kDa was detected in supernatants from brain and spinal cord, but not other tissues (Supplemental Fig. 2A). This is the only isoform of the five β-tubulin genes expressed in adult mammalian brain that is almost entirely neuron-specific (Lee et al., 1990). As shown in Fig. 5A, there was a significant reduction in relative β-tubulin class III levels per brain in D+aCSF and D+Ins *vs.* Non-D rats. This reduction was prevented in D+Ins+IGF, but not D+Ins *vs.* D +aCSF rats.

Neurofilaments are intermediate cytoskeletal proteins that determine the diameter of axons. Western blots showed one major ~68 kDa NF-L band that was shared between brain and spinal cord (Supplemental Fig. 2B). Four smaller bands shared with spinal cord were barely visible,

possibly represented degradation products, and were not quantified. Other tissues did not share these bands, indicating that these bands were selective for CNS tissues. There was a significant reduction in relative NF-L levels per brain in D+aCSF and D+Ins *vs.* Non-D rats (Fig. 5B). This reduction was prevented in D+Ins+IGF, but not D+Ins *vs.* D+aCSF rats.

A major NF-M band at ~160 kDa and two minor smaller bands were shared between brain and spinal cord supernatants (Supplemental Fig. 2C). None of these bands were present in other tissues, and the smaller bands may represent break-down products of NF-M. Only the major 160 kDa band was quantified. There was a significant decrease in relative levels of NF-M per brain in D+aCSF and D+Ins *vs.* Non-D rats (Fig. 5C). This decrease was prevented in D+Ins +IGF, but not D+Ins *vs.* D+aCSF rats.

2.6. The effect of diabetes, insulin, and the combination treatment on relative glial GFAP and PLP immunostaining in tissue slices from cortex and hippocampus

It was of interest to determine whether GFAP, PLP, NF-M, and β-tubulin class III levels were reduced in the hippocampal formation and cortex, brain regions that play an important role in learning and memory that is known to be impaired in diabetes. A separate group of rats was transcardially perfused with formaldehyde. The same antibodies used in Western blots were further used to immunostain Vibratome slices taken from regions of rat brain cingulate cortex and hippocampal formation. It should be considered that the small regions sampled for immunohistochemistry need not be representative of the average in the brain shown by the Western blot data. The cortex is a large brain structure and may show biochemical changes relatively close to the brain average, but this does not exclude the possibility for differences within regions of cortex. The relatively thick Vibratome slices permitted survey of a sizeable volume and representative data are shown taken generally from 3-4 slices.

The anti-GFAP antibodies prominently stained star-shaped astrocytes (arrowhead) and their processes in layer II (L2) of the cortex as well as in the molecular layer (ML), granule cell layer (GCL), and hilus (H) of the dentate gyrus (Fig. 6A). Astrocytic end-feet terminating on blood vessels were visible (asterisk). Immunoreactive GFAP levels associated with astrocytes (arrowhead) were visibly reduced in both cortex and particularly the hilus of the dentate in tissue sections from D+aCSF rats *vs.* Non-D rats. The reduced staining of astrocyte cell bodies and processes was consistent with the interpretation of atrophied cells with retracted end-feet in diabetes. The combination treatment prevented these changes such that astrocytes were essentially indistinguishable from normal. Insulin's effects seemed to be intermediate or resembled more the D+aCSF group. Reduction in GFAP immunoreactivity was widespread, because it was also observed in astrocytes from the granule cell layer as well as from radial glial cells in the molecular layer of the cerebellum from D+aCSF *vs.* Non-D, and such reduction was prevented in D+Ins+IGF rats (data not shown).

Oligodendrocyte myelin that tightly wraps around axons was stained heavily by anti-PLP antibodies in the cortex (arrowhead) and the three layers of the dentate gyrus in Non-D rat brains (Fig. 6B). The dense network of PLP-positive myelin associated with long axons in the cortex was sharply reduced in D+aCSF *vs.* Non-D rats. Immunostaining was reduced in the ML and hilus of the dentate from diabetic rats. PLP immunostaining was essentially normalized in the cortex and dentate gyrus of D+Ins+IGF rats. It was partially restored in the three layers of the dentate gyrus, but had no noticeable effect in the cortex of D+Ins rats.

2.7. Effect of diabetes, insulin, and the combination treatment on relative neuronal β-tubulin class III and NF-M immunostaining in tissue slices from cortex and hippocampus

It was of interest to determine whether the reductions in astrocyte- and oligodendrocyte-specific protein levels were associated with a similar reduction in immunostaining of cytoskeletal proteins comprising axons and dendrites in the cortex and hippocampal formation.

The anti-NF-M antibody stained a dense network of neurites (arrowhead) in the cortex of Non-D rats as shown in Fig. 7A; this network resembled that revealed by the anti-PLP immunostaining. The hilus and molecular layers of the dentate were heavily stained as well, but the density of neurites in the granule cell layer was lower (Fig. 7B). This is consistent with the observation that neurofilaments in the dentate are localized mainly to dendrites from parvalbumin-positive interneurons, but not granule cells (de Haas Ratzliff and Soltesz, 2000).

There was a qualitative reduction in NF-M immunostaining in the cortex and dentate gyrus in D+aCSF rats, and such reduction was prevented in the D+Ins+IGF group. Loss of immunostaining was prevented in the dentate, but not cortex in D+Ins rats.

Neuron-specific anti-β-tubulin class III antibodies abundantly stained a dense tangle of neurites (arrowhead) in the cortex of Non-D rats as shown in Fig. 7C, and in the striatum radiatum (SR) and pyramidal cell (PC) layers in the CA1 field of the hippocampus (Fig. 7D). Immunostaining was qualitatively reduced in both the cortex and CA1 field in D+aCSF rats, and such reduction was prevented in D+Ins+IGF and partially in the D+Ins rats. The dentate gyrus immunostaining was relatively unaffected by diabetes (not shown), suggesting regional differences.

Immunohistochemistry showed that the antibodies detected anticipated cell types and specific cellular structures. Taken together, diabetes caused reductions in GFAP, PLP, NF-M, and β-tubulin class III levels in cortex and hippocampus, and the combination prevented all of these changes. Insulin partially prevented changes, depending on region. These findings were complementary to the associated Western blot data.

2.8. CSF insulin levels

At conclusion of the experiment, CSF was tapped at cisterna magna and human insulin levels were measured by a sandwich ELISA. There was very little cross-reactivity of the test with endogenous rat insulin or rat IGF, and CSF did not otherwise interfere with the assay, as shown by the low signal in CSF samples from Non-D and D+aCSF rats (Fig. 8). The signal, while low, was not zero; 0.7% cross-occupancy with rat insulin and 0.02% with IGF was expected. There was a significant increase in CSF insulin levels in D+Ins and D+Ins+IGF *vs.* D+aCSF rats, showing that these treatments delivered human insulin into CSF.

2.9. Insulin and the combination treatment did not prevent hyperglycemia in plasma nor CSF of diabetic rats

Plasma glucose levels were elevated in all diabetic rat groups one day after the induction of diabetes (Fig. 9A), and remained so in all diabetic groups between weeks 2-12. At the conclusion of the experiment, CSF was withdrawn and glucose levels were assayed (Fig. 9B). CSF glucose means were significantly elevated in all diabetic groups *vs.* Non-D rats. D+Ins somewhat reduced CSF glucose levels *vs.* D+aCSF rats, although hyperglycemia per se was not prevented because the mean glucose levels remained above 11.1 mmol/L (200 mg/dL). Moreover, CSF glucose levels were not reduced in D+Ins+IGF rats, and these values were not different from D+Ins rats that received the same insulin dose. CSF was technically difficult to obtain and could not be withdrawn from all rats, so that CSF data from two separate experiments were pooled: (Non-D, 8 rats), (D+aCSF, 10), (D+Ins, 7) and (D+Ins+IGF, 9).

2.10. Insulin and the combination treatment did not prevent body weight loss nor kidney weight gain in diabetic rats

Insulin returned from the CSF into blood at the superior sagittal sinus may not be sufficiently high to modify plasma glucose levels, but it might still alter body or kidney weights, and this was examined. Rat body weights after 12 weeks were significantly lower in all diabetic rat groups *vs.* Non-D rats (Fig. 9C). Neither insulin nor its combination with IGF significantly changed body weights in diabetic rats. There was a significant increase in kidney wet weights in all diabetic rat groups *vs.* Non-D rats (Fig. 9D). This increase was not significantly reduced in D+Ins nor D+Ins+IGF *vs.* D+aCSF rats. Thus, kidney weights were elevated whereas brain weights were reduced, showing independent tissue weight regulation in diabetes.

3. Discussion

These data show that insulin and IGF prevented brain atrophy in diabetes. They prevented the loss of brain wet, dry, and water weights in an animal model with concomitantly reduced insulin and IGF levels. Insulin has two orders of magnitude lower affinity for IGF receptors, and its effects were not due to cross-occupancy of IGF receptors, else insulin's effects would have been essentially the same as those of the combination. The combination treatment virtually halted the loss of bulk brain DNA, total protein, and certain glial and neuronal proteins despite ongoing hyperglycemia and its secondary consequences. These data support the inference that insulin and IGF are factors that regulate adult brain mass. These studies have important implications because, as discussed below, brain atrophy associated with diabetes may be in large part a consequence of the concomitant decline in insulin and IGF levels.

It remains to be determined whether the effects of the combination are due to IGF-I alone or a synergistic action of insulin together with IGF-I. The subcutaneous administration of IGF-I to STZ diabetic rats prevented the impairment of learning and memory (Lupien et al., 2003), partially prevented the loss of brain protein content, but did not prevent the loss of bulk brain DNA nor brain atrophy (Lupien et al., 2006). Nevertheless, it remains possible that the higher CSF IGF-I concentration reached by its direct infusion into brain could account for the observed effects of the combination treatment in the present study. An experiment is underway to test this hypothesis.

STZ may potentially cause toxic effects including brain atrophy, independently of diabetes. However, the brain abnormalities found in diabetic rats were prevented by insulin or the combination treatment, and brain atrophy is observed in type 2 diabetic rats never exposed to STZ (Wuarin et al., 1996). These findings suggest that the observed brain abnormalities in diabetic rats are unlikely to be due to STZ toxicity.

3.1. Effect of insulin and the combination treatments on proteins associated with glia and neurons

Protein dysregulation in diabetic rats (discussed below) included disturbances in relatively abundant ubiquitous proteins as well as those selectively expressed in astrocytes, oligodendrocytes, and neurons. GFAP is expressed in astrocytes, whose end-feet envelop synapses or contact microvessels to affect blood-brain-barrier function, nutrient transport, and local hemodynamics (Schummers et al., 2008). GFAP levels are elevated early in experimental diabetes (Coleman et al., 2004), but are reduced at 6 weeks. TUNEL staining is co-localized with GFAP at 8 weeks in association with reduced astrocyte numbers (Lechuga-Sancho et al., 2006). Decreased GFAP levels and the potential effect of astrocyte dysfunction on neurons has been discussed (Coleman et al., 2004; Lechuga-Sancho et al., 2006). The present study showed a significant decline in total brain GFAP levels in diabetic rats that was partially prevented by insulin and completely by the combination treatment (Fig. 4A, 6A).

PLP comprises approximately 50% and MBP 30% of total myelin protein. Their levels were significantly reduced in diabetic rat brains, and those reductions were significantly prevented by insulin treatment (Fig. 4C, D). Immunohistochemical staining for PLP, associated with myelinated axons in the hippocampus and cortex, was visibly reduced in D+aCSF rats (Fig. 6 B); insulin partially and the combination more completely prevented these reductions. PLP and MBP mRNA and protein levels are reduced in diabetic rat brains (Kawashima et al., 2007), and MBP levels are reduced in the brain of diabetic patients (Palo et al., 1977). Although a reduction in MBP per protein was not observed in diabetic rats by Kawashima *et al.*, their myelin purification and expression of data as *MBP per protein* on gel lanes may attenuate differences between groups as discussed below.

Reduced levels of MBP and PLP may relate to disturbances in myelinated axons and glia that form the “white matter” of brain. White matter hyperintensities are lesions detected by MRI in types 1 and 2 diabetic patients (Brands et al., 2007; Dejgaard et al., 1991). Reduced myelin density (Sjobeck et al., 2005) and demyelination (Palo et al., 1977) may disrupt neural function, impair cognition, and reduce conduction velocity. Evoked central conduction velocities are reduced in diabetic patients.

Glutamine synthetase is expressed in both oligodendrocytes and astrocytes. Its content in diabetic rat brains was not significantly reduced (Fig. 4B). This result shows that some but not all proteins are regulated by insulin and its combination with IGF, and not all proteins are expected to have reduced levels in diabetes.

The combination treatment did, but insulin alone did not prevent the decline in neuron-specific β-tubulin class III, NF-L, and NF-M on Western blots (Fig. 5A, B, C). This same pattern was observed with another neuronal protein, glutaminase (unpublished observation). A decline in cytoskeletal proteins may reduce axonal and dendritic connectivity between neurons and impair neurotransmission. Neurofilament loss is observed in diabetic nerves (Schmidt et al., 1997).

Levels of ubiquitous structural proteins pan α-tubulin and pan β-tubulin were reduced in diabetes on Western blots (Fig. 3A, B); such reductions were prevented by the combination treatment, but not by insulin alone. The α- and β-tubulins form microtubules that are major cytoskeletal elements of axons and support axonal transport. The effects of insulin and IGF may be direct, because in cultured human neuroblastoma cells insulin and IGF both increase mRNA levels for α-tubulin, β-tubulin, NM-L, and NF-M during the induction of neurite outgrowth (Fernyhough et al., 1989; Wang et al., 1992). NF-L, NF-M, and α-tubulin mRNA levels are diminished in peripheral nerve ganglia in experimental diabetes (Mohiuddin et al., 1995).

The ubiquitous protein actin is involved in cell motility and is present in filopodia such as those located at axonal growth cones. Dendritic spines, structures believed to encode memory (Bailey and Kandel, 1993; Engert and Bonhoeffer, 1999), are enriched in actin, which regulates spine morphology and plasticity (Fifkova and Morales, 1992). The decrease in actin levels per brain in diabetic rats (Fig. 3A) may contribute to glial dysfunction, decreased neurites, and diminished plasticity of dendritic spines and synapses. The combination of insulin and IGF showed a trend to prevent this decrease, but insulin alone had no detectable effect.

The present immunohistochemical data showing reductions in GFAP, PLP, NF-M, and β-III tubulin do not distinguish whether there was cell atrophy with reduced antigen levels, cell loss, or both. Other investigators provide histochemical data indicative of cell atrophy as well as widespread brain cell death in rats 4-8 weeks after the induction of diabetes with STZ. Cleaved caspase-3 and TUNEL-stained cells are evident in the cortex, hippocampus (Britton et al., 2003; Rizk et al., 2005), preoptic area, hypothalamus (Britton et al., 2003), and cerebellum (Lechuga-Sancho et al., 2006). TUNEL staining co-localizes with GFAP in the latter study.

Light microscopy reveals dark neurons and foci of neuronal loss in the hippocampal formation, dentate gyrus, amygdala, thalamus, and hypothalamus (Piotrowski, 1999). Nuclear and perikaryon diameters are reduced in CA1, CA2, CA3, and the dentate gyrus (Piotrowski et al., 2001). The eye is formed as an out-pocketing of the brain, and IGF-I treatment prevents increased TUNEL staining in the neuroretina (Seigel et al., 2006). Further study will be needed to identify more completely the regions and cell types most susceptible to atrophy in diabetes and responsive to insulin and IGFs. Brain atrophy associated with a catabolic state presents challenges and caveats for the design and interpretation of future clinical and experimental studies on pathogenesis (see online Supplement).

The loss of total brain protein reflects the average of proteins unchanged, decreased, or possibly increased in diabetes; those decreased may be independent of or under regulation by insulin and IGFs. The relative decrease in neurofilaments and β-tubulin III after 12 weeks STZ diabetes may reflect their relative turnover rates and/or particular dependence on insulin/IGFs, and they may possibly contribute more heavily than most proteins to the decrease in total brain protein.

3.2. Associated deficits in electrophysiology and behavior

The immunohistochemistry for glial- and neuron-specific proteins suggests that there is associated fiber loss, and this might contribute to electrophysiological and behavioral disturbances observed 8-12 weeks after the induction of diabetes with STZ in rats. Evoked potentials (Ozkaya et al., 2007), centrally evoked forelimb motor responses (Emerick et al., 2005), and excitatory postsynaptic potentials (Kamal et al., 2006) are abnormal. Cognitive deficits are associated with abnormal long-term potentiation and long-term depression (Biessels et al., 1996; Biessels et al., 1998). Central nervous system conduction velocity is also reduced early in clinical diabetes (Donald et al., 1981; Pozzessere et al., 1988).

3.3. A catabolic state involving loss of proteins precedes brain degeneration

There is a significant reduction in total mRNA in brain 2 weeks after STZ-induced decreases in insulin and IGF levels (see Fig. 2C in ref. (Wuarin et al., 1996)). This is among the earliest known biochemical disturbances in the brain in diabetes. After 10 weeks, there is loss of total protein as well as mRNA per brain prior to measurable loss of DNA (unpublished data), and after 12 weeks there is loss of DNA together with reductions in 18S rRNA, total poly(A)$^+$ RNA, and total protein (Lupien et al., 2006). The present 12 week data also show loss of total DNA and protein per brain (Fig. 2D, E). The risk of brain degeneration is proposed to be greater with increasing severity and duration of the catabolic state (Lupien et al., 2006).

Insulin and IGF treatment prevented the catabolic state as well as brain atrophy and degeneration despite unabated hyperglycemia in plasma and CSF (Fig. 9A, B). The combination treatment prevented the loss of wet, water, dry weights, total protein, bulk DNA, and reductions in glia- and neuron-associated proteins. Body weight is a sensitive index of metabolic disturbance, and treatments did not correct the reduced body nor increased kidney weights in diabetic rats (Fig. 9C, D); brain mass was regulated independently of other tissues. These data show that brain atrophy and degeneration is predominantly due to insulin/IGF loss rather than hyperglycemia and its secondary consequences in brain.

IGF-I levels decline in the pre-diabetic state prior to frank diabetes (Bodkin et al., 1991), and IGF mRNA is directly regulated by insulin in cultured hepatic cells (Goya et al., 2001). On the other hand, IGF levels do not correlate with glucose levels (Bodkin et al., 1991; Tan and Baxter, 1986). This helps explain how IGF levels may be a risk factor for brain atrophy independently of hyperglycemia.

Other studies show that during unabated hyperglycemia in diabetic rats, subcutaneous IGF-I administration prevents impaired cognition (Lupien et al., 2003), partially the loss of brain protein content (Lupien et al., 2006), reduced brain IGF-II mRNA levels (Wuarin et al., 1996), and cell death in the neuroretina (Seigel et al., 2006). Together, these data support the hypothesis that insulin and IGF prevented the aforementioned aspects of brain degeneration predominantly through their growth factor rather than glucoregulatory pathways (Fig. 1).

The mean value of 173-211 mIU/ml in CSF from D+Ins and D+Ins+IGF rats (Fig. 8) was within the mid-range of insulin concentrations that are active on neurons. For example, 16.7 to 1670 mIU/ml (0.1 to 10 nM) insulin induces neurite outgrowth and supports protein synthesis in human neuroblastoma cells (Recio-Pinto and Ishii, 1984), increases neurite outgrowth in cultured rat sympathetic neurons (Recio-Pinto et al., 1986), and elevates α-tubulin, β-tubulin, NF-L and NF-M mRNA contents in human neuroblastoma cells (Wang et al., 1992). These data support the interpretation that brain atrophy and biochemical disturbances in diabetic rats were prevented by CSF insulin concentrations known to be active on neurons and within the physiological range. Because brain is <1% of the body weight of these rats, the >100-fold dilution of any CSF insulin spilling into peripheral blood at the superior sagittal sinus would deliver a blood insulin concentration much too low to prevent hyperglycemia in diabetic rats.

3.4. Signal transduction

Brain degeneration in adult rats is observed following local over-expression of a defective IGF-I receptor subunit that forms dimers with and inactivates endogenous brain IGF-I receptors (Carro et al., 2006). Because IGF-I receptor subunits can form hybrids with IR subunits, this treatment seems likely to also inactivate endogenous IRs, although this has not been studied. Insulin and IGF-I receptors are tyrosine kinases, and both can phosphorylate and activate IR substrate (IRS) proteins that in turn activate the ERK and PI3-kinase pathways. *Irs2*(-/-) mice have reduced brain size prior to onset of diabetes, whereas body size is near normal (Schubert et al., 2003). These data are consistent with the hypothesis that a concomitant reduction in insulin and IGF activity can cause brain atrophy. In contrast, brains are only moderately smaller in *Irs1*(-/-) mice, and this path may more selectively regulate body size. To what extent *Irs2* mediates atrophy in adult brain remains to be investigated.

3.5. Insulin actively regulates brain water content

Cerebral dehydration may develop with reduced insulin signaling in aging and diabetes. The cerebral edema that may emerge during clinical treatment of diabetic ketoacidosis has been attributed by some investigators to changes in the osmotic gradient between the brain and blood (Edge et al., 2006; Glaser et al., 2004). Insulin can induce a rapid decrease in glucose concentration in blood relative to the brain. This may cause passive movement of water down its concentration gradient into the CNS and contribute to potentially dangerous edema. However, insulin prevented the loss of brain water (Fig. 2) although it had no effect on the glucose gradient between CSF and plasma in diabetic rats (Fig. 9A, B). Insulin actively regulated water content, because it caused a flux of water from blood (relatively higher glucose and lower water concentration) into brain (relatively lower glucose and higher water concentration) against its own chemical gradient. Rapid or high dose insulin treatment in ketoacidosis may potentially cause elevated intracranial pressure due to active regulation of brain water content. The mechanism remains speculative, but may involve regulation of ion fluxes or aquaporins rather than an osmotic gradient.

3.6. Reduced Insulin and IGF Levels in Late-Onset Alzheimer's disease (LOAD)

There are other disorders in which brain atrophy and dementia are associated with concomitantly reduced insulin and IGF levels. Nearly 81% of LOAD cases had midlife diabetes or impaired fasting glucose (Janson et al., 2004; Razay and Wilcock, 1994). Cerebrospinal

fluid (CSF) insulin levels are decreased (Craft et al., 1998). In addition, circulating IGF levels are lower in LOAD patients than in age-matched normal subjects (Murialdo et al., 2001; Watanabe et al., 2005). Postmortem LOAD brains reveal a progressive decline in insulin and IR, as well as IGF and IGF-I receptor, mRNA levels (Rivera et al., 2005). Insulin treatment can enhance cognitive function in Alzheimer's patients (Reger et al., 2006), but it is unknown whether it can prevent brain atrophy. Further study of the relationship between the concomitant decrease in insulin and IGF levels and brain atrophy in LOAD as well as diabetes may be well worthwhile.

4. Experimental Procedures

4.1. Diabetic rat treatment

The NIH Guide for the Care and Use of Laboratory Animals was followed, and the animal protocol was approved by the Animal Care and Use Committee of Colorado State University. Wistar rats (275-300 g adult 11 week old males, Harlan Laboratories) were randomly assigned to treatment groups. Untreated rats were in the control group (Non-D, N = 8 rats), whereas STZ was used to induce type 1 diabetes in other rats as previously described (Lupien et al., 2003). STZ-treated rats with >20 mmol/L (360 mg/dL) glucose were enrolled in the study. Food and water were available ad libitum. Recombinant human IGF-I (Gropep, Australia) and human insulin (Sigma) were purchased. During the induction of diabetes, rats were deeply anesthetized with 110 mg/kg ketamine and 8 mg/kg xylazine i.p. and implanted subcutaneously in the mid-back with osmotic minipumps (Durect Corp., Cupertino, CA) that continuously released in 12 μl/day either 510 pmol/day insulin (D + Ins, N = 9), the combination of 510 pmol/day insulin plus 65 pmol/day of IGF-I (D + Ins + IGF, N = 9) or artificial cerebrospinal fluid (D + aCSF, N = 9) comprised of 10 mM NaCl, 1.8 mM $CaCl_2$, 1.2 mM $MgSO_4$, 2 mM K_2HPO_4, and 10 mM glucose, pH 7.4 for 12 weeks. These pumps were connected to a subcutaneous catheter that was routed to a cannula implanted into the brain left lateral ventricle (coordinates: -0.9 mm caudal and 1.5 mm left from bregma; 5 mm deep) using an Alzet Brain Infusion Kit (Durect Corp., Cupertino, CA). A rat stereotaxic instrument with micromanipulator and brain atlas were used (Paxinos and Watson, 1986). Buprenorphine 30 μg/kg was used beginning 1 day prior to and 3 days after surgery to provide postoperative analgesic care. At two week intervals, tail blood was withdrawn, and minipumps and solutions were replaced under brief isofluorane anesthesia. Correct placement in the ventricle was confirmed by injecting 20 μl dye through the catheter at time of assay. At the conclusion of the experiment, rats were weighed, deeply anesthetized with 110 mg/kg ketamine and 8 mg/kg xylazine, CSF withdrawn for glucose assays, then rats were euthanized with excess carbon dioxide while anesthetized. Kidney wet weights were measured. Various caveats and considerations guided these methods to study brain atrophy (see Supplement for details). The brain (except olfactory bulb) was separated from the spinal cord with a single perpendicular knife cut at the caudal edge of the cerebellum, and wet weights of brain were taken. Each brain was split down the midline and each brain half was weighed, frozen in liquid nitrogen, and stored at -70°C. Brain halves were homogenized with a Tissue Tearer (Fisher) in 10 ml of a buffer containing protease inhibitors: leupeptin, chymostatin, pepstatin A (all 10 μg/ml), and 0.1 mM phenylmethylsulfonylfluoride in 10 mM tris acetate and 5 mM EDTA, pH 7.4. Homogenates and all tissues were stored at -70°C.

4.2. Dry and water weights

Aliquots of tissue homogenates, taken after trituration 30 times, were lyophilized to measure dry weight in duplicate. The weight of an equivalent volume of buffer alone was subtracted from sample weights. The water content was the difference between tissue wet and dry weights.

4.3. DNA, protein, and glucose assays

Hoechst 33258 dye was added to an aliquot of brain homogenate. The dye bound to dsDNA was measured with a VersaFluor Fluorometer (Bio-Rad) (excitation 360 nm; emission 460 nm). Calf thymus DNA was used for concentration standard curves. Aliquots of tissue homogenates (after trituration 30 times) were solubilized with >1.4 g SDS/g protein and applied in duplicate to filter paper to measure protein content using a colorimetric dye-binding assay (Minamide and Bamburg, 1990). Bovine serum albumin was used to construct standard curves. Plasma and CSF glucose concentrations were measured using a glucose oxidase colorimetric assay (Sigma).

4.4. Western blots

Aliquots of brain homogenates taken after trituration 30 times were heated for 5 min at 40°C in gel loading buffer containing β-mercaptoethanol, 2% SDS and 4 M urea, and centrifuged at 10,000 × g for 30 min. Urea increased signal-to-noise ratios and reduced standard deviations. This treatment solubilized the samples for no precipitates nor cloudiness was visible prior to centrifugation, no pellet was visible, and aliquots of the supernatant solutions were used for Western blots. Certain standard Western blotting protocols may be inappropriate where there is brain atrophy. For example, the same amount of protein may be loaded per gel lane, but this is questionable in diabetes where total protein levels are reduced. Levels of antigens on Western blots are often reported relative to total brain protein, actin levels, wet weights, or DNA. Yet the levels of all of these normalization parameters are changed in brain atrophy (see Results). Suppose that the left cortex, or every second brain cell, were completely lost but remaining brain cells were otherwise healthy. None of the forgoing standard protocols are likely to detect these losses. To avoid such concerns, present Western blot results were expressed on a per brain basis (see Methods). To accommodate all samples, four gels were simultaneously run in a Mini-PROTEAN Tetra Cell (Bio-Rad), and three lanes of each gel contained a Non-D normalization standard. The mean signal intensity of the three standards was used to normalize values between the four blots. Following SDS-PAGE, samples were transferred to Immobilon-P^{sq} PVDF membranes (Millipore) using a Trans-Blot SD Cell (Bio-Rad). For each primary antibody, a two-fold serial dilution of the SDS/urea supernatant from a Non-D rat was used to determine the linear and non-saturating range for studies. The following primary antibodies were used in 3% BSA/TBST: rabbit anti-glial fibrillary acidic protein (GFAP) polyclonal immunoglobulins (1:2,000 Z0334, DakoCytomation) as well as rabbit anti-myelin basic protein (MBP) polyclonal (1:3,000 AB980 Chemicon), mouse anti-proteolipid protein (PLP) (1:750 clone MAB388 Chemicon), mouse anti-glutamine synthetase (1:2,000 MAB302 Chemicon), mouse anti-actin (1:2,700 clone C4 Chemicon), and mouse anti-β-tubulin class III (1:830, clone TU-20 Chemicon), mouse anti-neurofilament light (NF-L) (1:1,000 Clone NR4, Sigma), mouse anti-neurofilament medium (NF-M) (1:1,000 Clone NN18, Sigma), mouse anti-α-tubulin (1:2,000 clone DM1A, Upstate), and mouse anti-β-tubulin (1:1,750 clone AA2, Upstate). Tissue specificity studies (15 μg/lane non-diabetic rat brain, spinal cord, liver, intestine, heart and kidney) were conducted with the same dilution of primary antibodies used in the Western blot studies (see Supplementary Material, online).

Goat anti-rabbit or anti-mouse IgG coupled to AlexaFluor680 (Invitrogen) were diluted 1:10,000 in 3% BSA/TBST and used as secondary antibodies. The Odyssey InfraRed Imaging System (LI-COR Biosciences) with signal intensities that are linear over up to five orders of magnitude was used to capture images and analyze results. The average background from at least four equal size areas from gel lanes was subtracted from the signal from each band of interest. For example, for a sample run on gel 2, the sample value per brain was calculated as (sample signal intensity − avg. membrane 2 background) × [(avg. Non-D normalization standards on membrane 1)/(avg. Non-D normalization standards on membrane 2)] × (total brain homogenate volume)/(sample homogenate volume). The results from two or more

replicate electrophoresis runs were averaged, and values were reported as relative group means per brain ± s.e.m.

4.5. Immunohistochemistry

At the end of 12 weeks, a separate group of rats was deeply anesthetized with ketamine/xylazine, then subjected to transcardiac perfusion with 0.9% saline to remove blood from tissues, followed by ice-cold 4% paraformaldehyde in 0.1 M PBS. Following a mid-line saggital cut and coronal division into 4 mm blocks using a rat brain matrix (Kent Scientific, Torrington, CT), the fragments were stored in cold 4% paraformaldehyde in 0.1 M PBS for 2 months, in cold 70% ethanol for 2 months, then in 1% paraformaldehyde until used. A rat brain stereotaxic atlas was used for survey purposes. Vibratome 50 μm floating coronal hemisections from rat groups were incubated with the same primary antibody used for the Western blots, then processed simultaneously. Sections were incubated for 30 min in 5% normal goat serum for rabbit primary antibodies or 5% normal horse serum for mouse primary antibodies in phosphate buffered saline (PBS, Sigma) containing 0.3% Triton X-100 and 3% peroxide. Primary antibodies were used at the following dilutions: anti-GFAP (1:1,000), anti-PLP (1:3,000), anti β-tubulin class III (1:4,000) and anti-NF-M (1:2,000). Sections were incubated in the primary antibody diluted in PBS overnight at room temperature with agitation. On the following day, slices were washed with PBS, then incubated for 1 h in biotinylated goat anti-rabbit or horse anti-mouse IgG (Vector Laboratories) diluted 1:200 in PBS. Sections were washed again in PBS and further incubated for 1 h with avidin-biotinylated peroxidase (ABC Reagent, Vectastain Elite kit), rinsed thoroughly and diaminobenzidine was used as a substrate chromogen. After a final wash in PBS, slices were mounted on Superfrost Plus slides, air-dried, cleared in xylene and cover slip added using Accumount 60 (Baxter Scientific Products, McGraw Park, IL). Slides were observed under brightfield illumination with neutral density filters 6 and 12 under a 40× objective using a Zeiss Axioplan 2 microscope, and images of areas of interest were captured at the same illumination using an AxioCam CCD camera and AxioVision v4.6 software (Carl Zeiss, Inc., Thornwood, NY). Images were processed and figures assembled using Adobe Photoshop 6.0 software.

4.6. Insulin ELISA

Two different monoclonal antibodies, each directed at a separate site on the human insulin molecule, were used in the sandwich Ultrasensitive Insulin ELISA test that used 3,3′-5,5′ tetramethylbenzidine as the peroxidase substrate (Mercodia AB, Sweden). Cross-reactivity against C-peptide < 0.01%, proinsulin < 0.01%, hIGF-I < 0.02%, hIGF-II < 0.02%, and rat insulin < 0.7%. Rat CSF samples were diluted 1:40 prior to test according to manufacturer's specifications. OD450 nm was measured in a 96 microwell plate reader (Bio-Rad).

4.7. Statistical Analysis

A software program was used for statistical analysis (SAS V9.1.3). For purposes of comparing multiple group means, an ANOVA Tukey-Kramer posthoc two-tailed test was used, and significance was accepted at $P<0.05$. The values are group means ± s.e.m.

Supplementary Material

Refer to Web version on PubMed Central for supplementary material.

Acknowledgments

This work was supported by Centers for Disease Control and Prevention Grant R49/CCR811509, and Colorado Commission on Higher Education Technology Advancement Grant TAG 06-01. P.S. was supported in part by NIH Training Grant NS43115. A preliminary account of this study appeared as: Bluhm, E.J., Brownson-Randolph, E. and

Ishii, D.N., 2005. Insulin Levels Rather Than Hyperglycemia Regulate Brain Atrophy in A Rat Model of Diabetic Dementia. Soc Neurosci. Abs # 106.26.

Many thanks to Drs. James R. Bamburg, Norman P. Curthoys, and Stuart A. Tobet for their encouragement and insightful comments during the course of these studies. We thank students Dana Rioux-Forker, Mark C. Goodwin II, Daniel Kipp, and Shana E. Nelson for technical assistance. Erik J. Bluhm, who passed away during the course of these studies, contributed to the early stages of this project. We are greatly saddened by the loss of this engaging young graduate student.

DNI has submitted a series of patent applications through the Colorado State University Research Foundation beginning prior to 1996 concerning the use of insulin and IGFs to treat neurodegenerative disorders. He is Founder and stockholder of Aurogen Inc which has licensed rights to these patents and applications. Other authors have no disclosures to report.

References

Araki Y, Nomura M, Tanaka H, Yamamoto H, Yamamoto T, Tsukaguchi I, Nakamura H. MRI of the brain in diabetes mellitus. Neuroradiology 1994;36:101–3. [PubMed: 8183443]

Bailey CH, Kandel ER. Structural changes accompanying memory storage. Annu Rev Physiol 1993;55:397–426. [PubMed: 8466181]

Biessels GJ, Kamal A, Ramakers GM, Urban IJ, Spruijt BM, Erkelens DW, Gispen WH. Place learning and hippocampal synaptic plasticity in streptozotocin-induced diabetic rats. Diabetes 1996;45:1259–66. [PubMed: 8772732]

Biessels GJ, Kamal A, Urban IJ, Spruijt BM, Erkelens DW, Gispen WH. Water maze learning and hippocampal synaptic plasticity in streptozotocin-diabetic rats: effects of insulin treatment. Brain Res 1998;800:125–35. [PubMed: 9685609]

Bodkin NL, Sportsman R, DiMarchi RD, Hansen BC. Insulin-like growth factor-I in non-insulin-dependent diabetic monkeys: basal plasma concentrations and metabolic effects of exogenously administered biosynthetic hormone. Metabolism 1991;40:1131–7. [PubMed: 1943741]

Brands AM, Biessels GJ, Kappelle LJ, de Haan EH, de Valk HW, Algra A, Kessels RP. Cognitive functioning and brain MRI in patients with type 1 and type 2 diabetes mellitus: a comparative study. Dement Geriatr Cogn Disord 2007;23:343–50. [PubMed: 17374953]

Britton M, Rafols J, Alousi S, Dunbar JC. The effects of middle cerebral artery occlusion on central nervous system apoptotic events in normal and diabetic rats. Int J Exp Diabesity Res 2003;4:13–20. [PubMed: 12745666]

Bruning JC, Gautam D, Burks DJ, Gillette J, Schubert M, Orban PC, Klein R, Krone W, Muller-Wieland D, Kahn CR. Role of brain insulin receptor in control of body weight and reproduction. Science 2000;289:2122–5. [PubMed: 11000114]

Busiguina S, Fernandez AM, Barrios V, Clark R, Tolbert DL, Berciano J, Torres-Aleman I. Neurodegeneration is associated to changes in serum insulin-like growth factors. Neurobiol Dis 2000;7:657–65. [PubMed: 11114263]

Carro, E.; Trejo, JL.; Spuch, C.; Bohl, D.; Heard, JM.; Torres-Aleman, I. Neurobiol Aging. Vol. 27. 2006. Blockade of the insulin-like growth factor I receptor in the choroid plexus originates Alzheimer's-like neuropathology in rodents: new cues into the human disease?; p. 1618-31.

Coleman E, Judd R, Hoe L, Dennis J, Posner P. Effects of diabetes mellitus on astrocyte GFAP and glutamate transporters in the CNS. Glia 2004;48:166–78. [PubMed: 15378652]

Craft S, Peskind E, Schwartz MW, Schellenberg GD, Raskind M, Porte D Jr. Cerebrospinal fluid and plasma insulin levels in Alzheimer's disease: relationship to severity of dementia and apolipoprotein E genotype. Neurology 1998;50:164–8. [PubMed: 9443474]

Cukierman T, Gerstein HC, Williamson JD. Cognitive decline and dementia in diabetes--systematic overview of prospective observational studies. Diabetologia 2005;48:2460–9. [PubMed: 16283246]

de Haas Ratzliff A, Soltesz I. Differential expression of cytoskeletal proteins in the dendrites of parvalbumin-positive interneurons versus granule cells in the adult rat dentate gyrus. Hippocampus 2000;10:162–8. [PubMed: 10791838]

Dejgaard A, Gade A, Larsson H, Balle V, Parving A, Parving HH. Evidence for diabetic encephalopathy. Diabet Med 1991;8:162–7. [PubMed: 1827403]

den Heijer T, Vermeer SE, van Dijk EJ, Prins ND, Koudstaal PJ, Hofman A, Breteler MM. Type 2 diabetes and atrophy of medial temporal lobe structures on brain MRI. Diabetologia 2003;46:1604–10. [PubMed: 14595538]

Donald MW, Bird CE, Lawson JS, Letemendia FJ, Monga TN, Surridge DH, Varette-Cerre P, Williams DL, Williams DM, Wilson DL. Delayed auditory brainstem responses in diabetes mellitus. J Neurol Neurosurg Psychiatry 1981;44:641–4. [PubMed: 7288453]

Edge JA, Jakes RW, Roy Y, Hawkins M, Winter D, Ford-Adams ME, Murphy NP, Bergomi A, Widmer B, Dunger DB. The UK case-control study of cerebral oedema complicating diabetic ketoacidosis in children. Diabetologia 2006;49:2002–9. [PubMed: 16847700]

Emerick AJ, Richards MP, Kartje GL, Neafsey EJ, Stubbs EB Jr. Experimental diabetes attenuates cerebral cortical-evoked forelimb motor responses. Diabetes 2005;54:2764–71. [PubMed: 16123367]

Engert F, Bonhoeffer T. Dendritic spine changes associated with hippocampal long-term synaptic plasticity. Nature 1999;399:66–70. [PubMed: 10331391]

Fernyhough P, Mill JF, Roberts JL, Ishii DN. Stabilization of tubulin mRNAs by insulin and insulin-like growth factor I during neurite formation. Brain Res Mol Brain Res 1989;6:109–20. [PubMed: 2693875]

Fifkova E, Morales M. Actin matrix of dendritic spines, synaptic plasticity, and long-term potentiation. Int Rev Cytol 1992;139:267–307. [PubMed: 1428678]

Fox MA, Chen RS, Holmes CS. Gender differences in memory and learning in children with insulin-dependent diabetes mellitus (IDDM) over a 4-year follow-up interval. J Pediatr Psychol 2003;28:569–78. [PubMed: 14602847]

Glaser NS, Wootton-Gorges SL, Marcin JP, Buonocore MH, Dicarlo J, Neely EK, Barnes P, Bottomly J, Kuppermann N. Mechanism of cerebral edema in children with diabetic ketoacidosis. J Pediatr 2004;145:164–71. [PubMed: 15289761]

Goya L, de la Puente A, Ramos S, Martin MA, Escriva F, Alvarez C, Pascual-Leone AM. Regulation of IGF-I and -II by insulin in primary cultures of fetal rat hepatocytes. Endocrinology 2001;142:5089–96. [PubMed: 11713201]

Janson J, Laedtke T, Parisi JE, O'Brien P, Petersen RC, Butler PC. Increased risk of type 2 diabetes in Alzheimer disease. Diabetes 2004;53:474–81. [PubMed: 14747300]

Kamal A, Biessels GJ, Gispen WH, Ramakers GM. Synaptic transmission changes in the pyramidal cells of the hippocampus in streptozotocin-induced diabetes mellitus in rats. Brain Res 2006;1073-1074:276–80. [PubMed: 16455062]

Kawashima R, Kojima H, Nakamura K, Arahata A, Fujita Y, Tokuyama Y, Saito T, Furudate S, Kurihara T, Yagishita S, Kitamura K, Tamai Y. Alterations in mRNA expression of myelin proteins in the sciatic nerves and brains of streptozotocin-induced diabetic rats. Neurochem Res 2007;32:1002–10. [PubMed: 17404843]

Lechuga-Sancho AM, Arroba AI, Frago LM, Paneda C, Garcia-Caceres C, Delgado Rubin de Celix A, Argente J, Chowen JA. Activation of the intrinsic cell death pathway, increased apoptosis and modulation of astrocytes in the cerebellum of diabetic rats. Neurobiol Dis 2006;23:290–9. [PubMed: 16753303]

Lee MK, Tuttle JB, Rebhun LI, Cleveland DW, Frankfurter A. The expression and posttranslational modification of a neuron-specific beta-tubulin isotype during chick embryogenesis. Cell Motil Cytoskeleton 1990;17:118–32. [PubMed: 2257630]

Lunetta M, Damanti AR, Fabbri G, Lombardo M, Di Mauro M, Mughini L. Evidence by magnetic resonance imaging of cerebral alterations of atrophy type in young insulin-dependent diabetic patients. J Endocrinol Invest 1994;17:241–5. [PubMed: 7930374]

Lupien SB, Bluhm EJ, Ishii DN. Systemic insulin-like growth factor-I administration prevents cognitive impairment in diabetic rats, and brain IGF regulates learning/memory in normal adult rats. J Neurosci Res 2003;74:512–23. [PubMed: 14598295]

Lupien SB, Bluhm EJ, Ishii DN. Effect of IGF-I on DNA, RNA, and protein loss associated with brain atrophy and impaired learning in diabetic rats. Neurobiol Dis 2006;21:487–95. [PubMed: 16181784]

Minamide LS, Bamburg JR. A filter paper dye-binding assay for quantitative determination of protein without interference from reducing agents or detergents. Anal Biochem 1990;190:66–70. [PubMed: 2285147]

Mohiuddin L, Fernyhough P, Tomlinson DR. Reduced levels of mRNA encoding endoskeletal and growth-associated proteins in sensory ganglia in experimental diabetes. Diabetes 1995;44:25–30. [PubMed: 7813810]

Murialdo G, Barreca A, Nobili F, Rollero A, Timossi G, Gianelli MV, Copello F, Rodriguez G, Polleri A. Relationships between cortisol, dehydroepiandrosterone sulphate and insulin-like growth factor-I system in dementia. J Endocrinol Invest 2001;24:139–46. [PubMed: 11314741]

Olchovsky D, Bruno JF, Wood TL, Gelato MC, Leidy JW Jr, Gilbert JM Jr, Berelowitz M. Altered pituitary growth hormone (GH) regulation in streptozotocin-diabetic rats: a combined defect of hypothalamic somatostatin and GH-releasing factor. Endocrinology 1990;126:53–61. [PubMed: 1967164]

Ott A, Stolk RP, van Harskamp F, Pols HA, Hofman A, Breteler MM. Diabetes mellitus and the risk of dementia: The Rotterdam Study. Neurology 1999;53:1937–42. [PubMed: 10599761]

Ozkaya YG, Agar A, Hacioglu G, Yargicoglu P. Exercise improves visual deficits tested by visual evoked potentials in streptozotocin-induced diabetic rats. Tohoku J Exp Med 2007;213:313–21. [PubMed: 18075235]

Palo J, Reske-Nielsen E, Riekkinen P. Enzyme and protein studies of demyelination in diabetes. J Neurol Sci 1977;33:171–8. [PubMed: 71340]

Paxinos, G.; Watson, C. The rat brain in stereotaxic coordinates, Vol. Academic Press; Sydney; Orlando: 1986.

Perros P, Deary IJ, Sellar RJ, Best JJ, Frier BM. Brain abnormalities demonstrated by magnetic resonance imaging in adult IDDM patients with and without a history of recurrent severe hypoglycemia. Diabetes Care 1997;20:1013–8. [PubMed: 9167117]

Piotrowski P. Morphology of experimental diabetes and cerebral ischemia in the rat brain. Folia Neuropathol 1999;37:252–5. [PubMed: 10705647]

Piotrowski P, Wierzbicka K, Smialek M. Neuronal death in the rat hippocampus in experimental diabetes and cerebral ischaemia treated with antioxidants. Folia Neuropathol 2001;39:147–54. [PubMed: 11770125]

Pozzessere G, Rizzo PA, Valle E, Mollica MA, Meccia A, Morano S, Di Mario U, Andreani D, Morocutti C. Early detection of neurological involvement in IDDM and NIDDM. Multimodal evoked potentials versus metabolic control. Diabetes Care 1988;11:473–80. [PubMed: 3402302]

Prescott JH, Richardson JT, Gillespie CR. Cognitive function in diabetes mellitus: the effects of duration of illness and glycaemic control. Br J Clin Psychol 1990;29(Pt 2):167–75. [PubMed: 2364194]

Pulford BE, Ishii DN. Uptake of circulating insulin-like growth factors (IGFs) into cerebrospinal fluid appears to be independent of the IGF receptors as well as IGF-binding proteins. Endocrinology 2001;142:213–20. [PubMed: 11145584]

Razay G, Wilcock GK. Hyperinsulinaemia and Alzheimer's disease. Age Ageing 1994;23:396–9. [PubMed: 7825486]

Recio-Pinto E, Ishii DN. Effects of insulin, insulin-like growth factor-II and nerve growth factor on neurite outgrowth in cultured human neuroblastoma cells. Brain Res 1984;302:323–34. [PubMed: 6329460]

Recio-Pinto E, Rechler MM, Ishii DN. Effects of insulin, insulin-like growth factor-II, and nerve growth factor on neurite formation and survival in cultured sympathetic and sensory neurons. J Neurosci 1986;6:1211–9. [PubMed: 3519887]

Reger MA, Watson GS, Frey WH 2nd, Baker LD, Cholerton B, Keeling ML, Belongia DA, Fishel MA, Plymate SR, Schellenberg GD, Cherrier MM, Craft S. Effects of intranasal insulin on cognition in memory-impaired older adults: modulation by APOE genotype. Neurobiol Aging 2006;27:451–8. [PubMed: 15964100]

Reske-Nielsen E, Lundbaek K. Diabetic Encephalopathy. Diffuse and Focal Lesions of the Brain in Long-Term Diabetes. Acta Neurol Scand Suppl 1963;39:273–90. [PubMed: 14057514]

Rivera EJ, Goldin A, Fulmer N, Tavares R, Wands JR, de la Monte SM. Insulin and insulin-like growth factor expression and function deteriorate with progression of Alzheimer's disease: link to brain reductions in acetylcholine. J Alzheimers Dis 2005;8:247–68. [PubMed: 16340083]

Rizk NN, Rafols J, Dunbar JC. Cerebral ischemia induced apoptosis and necrosis in normal and diabetic rats. Brain Res 2005;1053:1–9. [PubMed: 16038884]

Rollero A, Murialdo G, Fonzi S, Garrone S, Gianelli MV, Gazzerro E, Barreca A, Polleri A. Relationship between cognitive function, growth hormone and insulin-like growth factor I plasma levels in aged subjects. Neuropsychobiology 1998;38:73–9. [PubMed: 9732206]

Ryan CM, Williams TM, Finegold DN, Orchard TJ. Cognitive dysfunction in adults with type 1 (insulin-dependent) diabetes mellitus of long duration: effects of recurrent hypoglycaemia and other chronic complications. Diabetologia 1993;36:329–34. [PubMed: 8477878]

Schmidt RE, Beaudet LN, Plurad SB, Dorsey DA. Axonal cytoskeletal pathology in aged and diabetic human sympathetic autonomic ganglia. Brain Res 1997;769:375–83. [PubMed: 9374210]

Schubert M, Brazil DP, Burks DJ, Kushner JA, Ye J, Flint CL, Farhang-Fallah J, Dikkes P, Warot XM, Rio C, Corfas G, White MF. Insulin receptor substrate-2 deficiency impairs brain growth and promotes tau phosphorylation. J Neurosci 2003;23:7084–92. [PubMed: 12904469]

Schubert M, Gautam D, Surjo D, Ueki K, Baudler S, Schubert D, Kondo T, Alber J, Galldiks N, Kustermann E, Arndt S, Jacobs AH, Krone W, Kahn CR, Bruning JC. Role for neuronal insulin resistance in neurodegenerative diseases. Proc Natl Acad Sci U S A 2004;101:3100–5. [PubMed: 14981233]

Schummers J, Yu H, Sur M. Tuned responses of astrocytes and their influence on hemodynamic signals in the visual cortex. Science 2008;320:1638–43. [PubMed: 18566287]

Seigel GM, Lupien SB, Campbell LM, Ishii DN. Systemic IGF-I treatment inhibits cell death in diabetic rat retina. J Diabetes Complications 2006;20:196–204. [PubMed: 16632241]

Sjobeck M, Haglund M, Englund E. Decreasing myelin density reflected increasing white matter pathology in Alzheimer's disease--a neuropathological study. Int J Geriatr Psychiatry 2005;20:919–26. [PubMed: 16163742]

Tan K, Baxter RC. Serum insulin-like growth factor I levels in adult diabetic patients: the effect of age. J Clin Endocrinol Metab 1986;63:651–5. [PubMed: 3734035]

Wang C, Li Y, Wible B, Angelides KJ, Ishii DN. Effects of insulin and insulin-like growth factors on neurofilament mRNA and tubulin mRNA content in human neuroblastoma SH-SY5Y cells. Brain Res Mol Brain Res 1992;13:289–300. [PubMed: 1320719]

Watanabe T, Miyazaki A, Katagiri T, Yamamoto H, Idei T, Iguchi T. Relationship between serum insulin-like growth factor-1 levels and Alzheimer's disease and vascular dementia. J Am Geriatr Soc 2005;53:1748–53. [PubMed: 16181175]

Woods SC, Seeley RJ, Baskin DG, Schwartz MW. Insulin and the blood-brain barrier. Curr Pharm Des 2003;9:795–800. [PubMed: 12678878]

Wuarin L, Namdev R, Burns JG, Fei ZJ, Ishii DN. Brain insulin-like growth factor-II mRNA content is reduced in insulin-dependent and non-insulin-dependent diabetes mellitus. J Neurochem 1996;67:742–51. [PubMed: 8764603]

Abbreviations

aCSF	artificial cerebrospinal fluid
CSF	cerebrospinal fluid
D+aCSF	diabetic rats infused i.c.v. with aCSF
D+Ins	diabetic rats infused with insulin
D+Ins+IGF	diabetic rats infused with both insulin and IGF
GFAP	glial fibrillary acidic protein
IGF	insulin-like growth factor
IR	insulin receptor
LOAD	late-onset Alzheimer's disease

MBP	myelin basic protein
NF-L	neurofilament light
NF-M	neurofilament medium
Non-D	non-diabetic control rats
PLP	proteolipid protein
STZ	streptozotocin

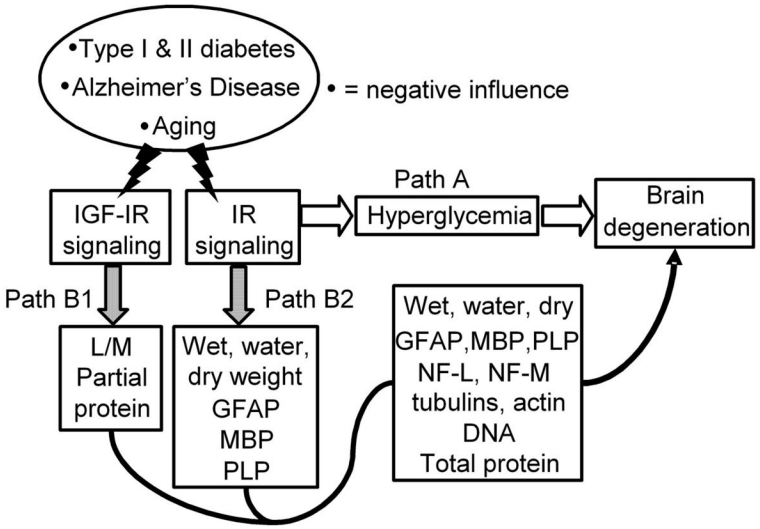

Fig. 1.

Two hypotheses for the pathogenesis of adult brain atrophy and degeneration due to concomitantly reduced signaling through the insulin as well as IGF systems. Insulin and IGF signaling are reduced with aging and further as a consequence of type 1 diabetes, type 2 diabetes or Alzheimer's disease.

"Classical" hypothesis: Reduced IR signaling via Path A glucoregulatory activity leads to hyperglycemia, increased polyol levels, accumulation of advanced glycation end (AGE) products, abnormal protein glycosylation, hyperlipemia, dehydration and other metabolic consequences that are widely believed to be pathogenic for brain atrophy and degeneration.

Alternative hypothesis: The IR signals simultaneously via Path A glucoregulatory and Path B growth factor activities. It is proposed that a *concomitant* decline in insulin system and IGF system signaling results in a catabolic state in brain by predominantly, albeit not necessarily exclusively, the loss of Path B growth factor activities relatively independent of Path A glucoregulation. IR signaling *via* Path B1 prevents the loss of brain wet, water and dry weights as well as glial fibrillary acidic protein (GFAP), myelin basic protein (MBP), and proteolipid protein (PLP) levels. IGF-I receptor signaling prevents the loss of learning and memory and partially the loss of brain protein content via Path B2 (Lupien et al., 2003). The combination of insulin and IGF may regulate brain wet, water, dry weights, DNA, total protein, GFAP, PLP, NF-L, NF-M, β-tubulin class III, α-tubulin and β-tubulin contents. The existence of Path B can be tested by the *discriminating prediction* that a tiny local *i.c.v.* dose of insulin or its combination with IGF can prevent brain atrophy and degeneration independently of unabated Path A hyperglycemia in diabetic rats.

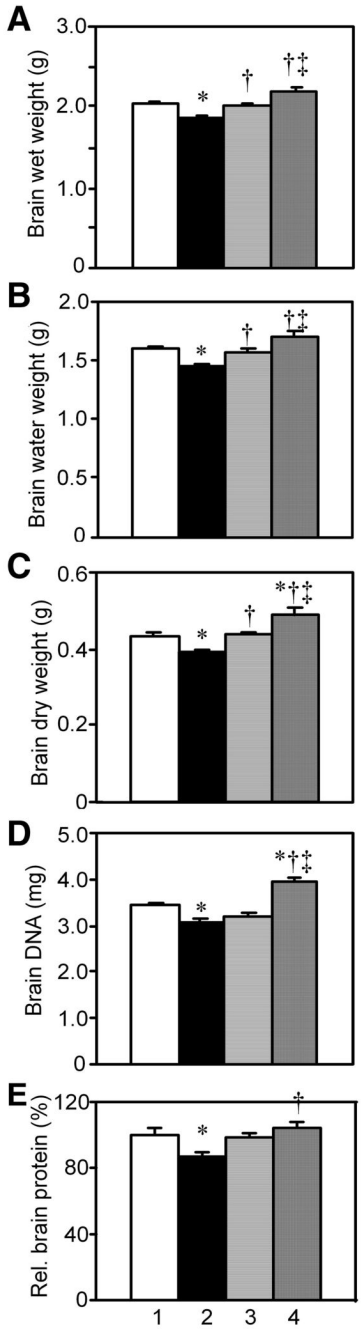

Fig. 2.

The effect of diabetes, insulin or its combination with IGF on brain wet, water and dry weights, DNA per brain, and total relative protein content per brain. Diabetes was induced with STZ in adult rats, and beginning immediately thereafter either insulin (D+Ins), a combination of insulin and IGF (D+Ins+IGF) or artificial CSF (D+aCSF) was infused into the brain lateral ventricles for 12 weeks. Lane 1, Non-D; Lane 2, D+aCSF; Lane 3, D+Ins; and Lane 4, D+Ins+IGF. Values are group means ± s.e.m. P values showing statistical comparisons for all figures are summarized in Table 1. **A.** Brain wet weights. Brain homogenates were prepared from which aliquots were used to measure water and dry weights as well as DNA and protein contents.

B. Brain water weights. **C.** Brain dry weights. **D.** DNA per brain. **E.** Relative protein content per brain.

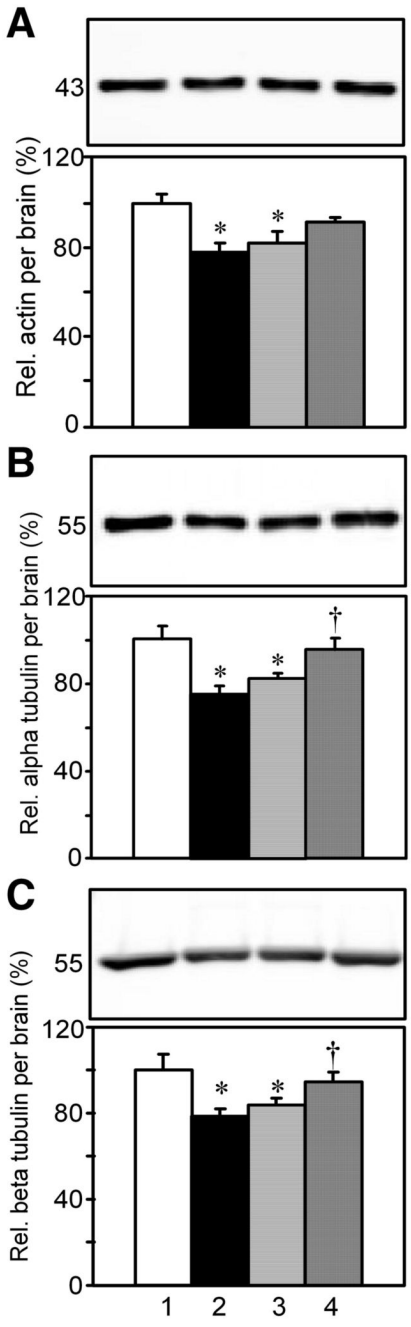

Fig. 3.

The effect of diabetes, insulin, or its combination with IGF on the relative levels of the ubiquitous proteins actin, α-tubulins, and β-tubulins per brain. SDS/urea 10,000×g supernatant brain extracts were subjected to SDS-PAGE and Western blots. The upper panels shows representative bands on Western blots, and the lower panels show group means ± s.e.m. Lane 1, Non-D; Lane 2, D+aCSF; Lane 3, D+Ins; and Lane 4, D+Ins+IGF. **A.** Relative pan-actin levels per brain. **B.** Pan α-tubulin levels per brain. **C.** Pan β-tubulin levels per brain.

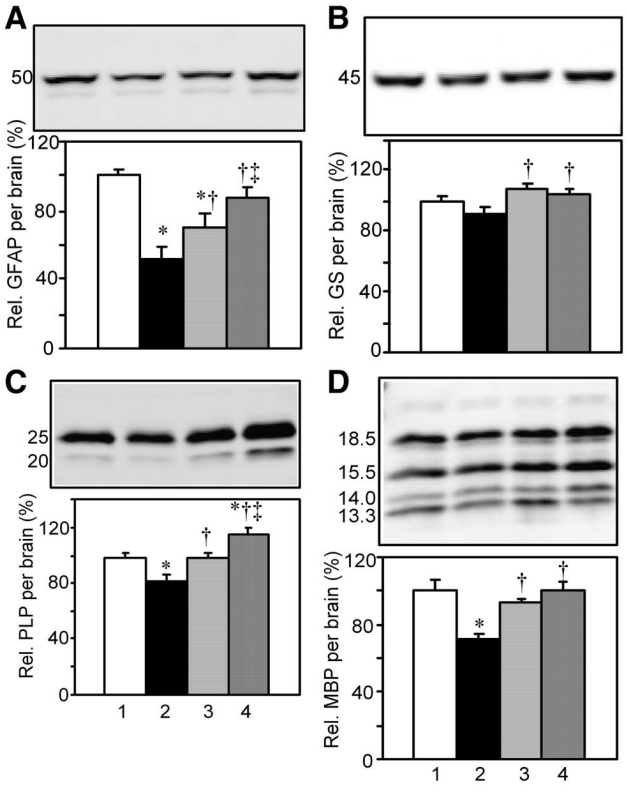

Fig. 4.

The effect of diabetes, insulin, or its combination with IGF on relative glial GFAP, GS, PLP, and MBP levels per brain. Method same as Fig. 3. **A.** Relative GFAP levels per brain. **B.** Relative glutamine synthetase levels per brain. **C.** Relative PLP levels per brain. **D.** Relative MBP levels per brain.

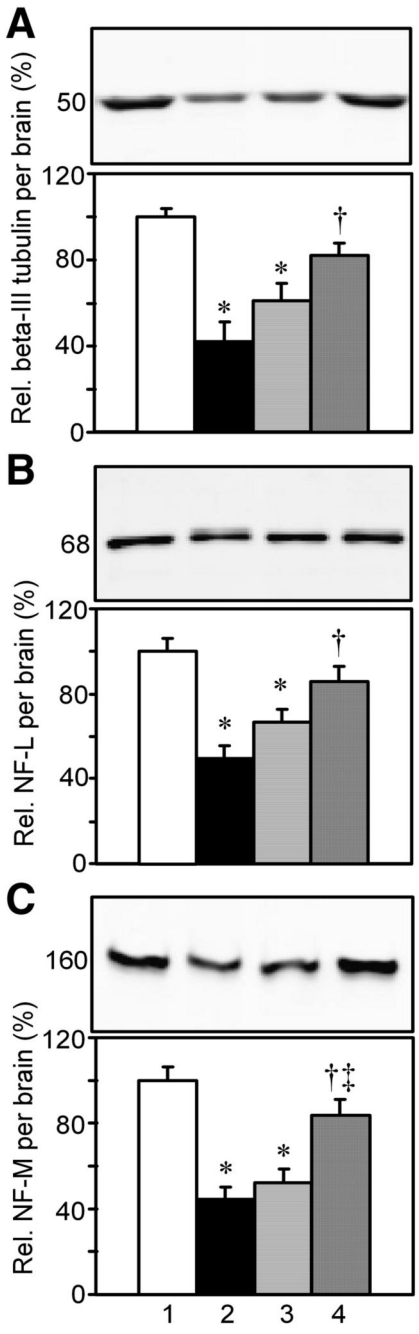

Fig. 5.

The effect of diabetes, insulin, or its combination with IGF on relative neuronal β-tubulin class III, NF-L, and NF-M levels per brain. Method same as Fig. 3. **A.** Relative β-tubulin class III levels per brain. **B.** Relative NF-L levels per brain. **C.** Relative NF-M levels per brain.

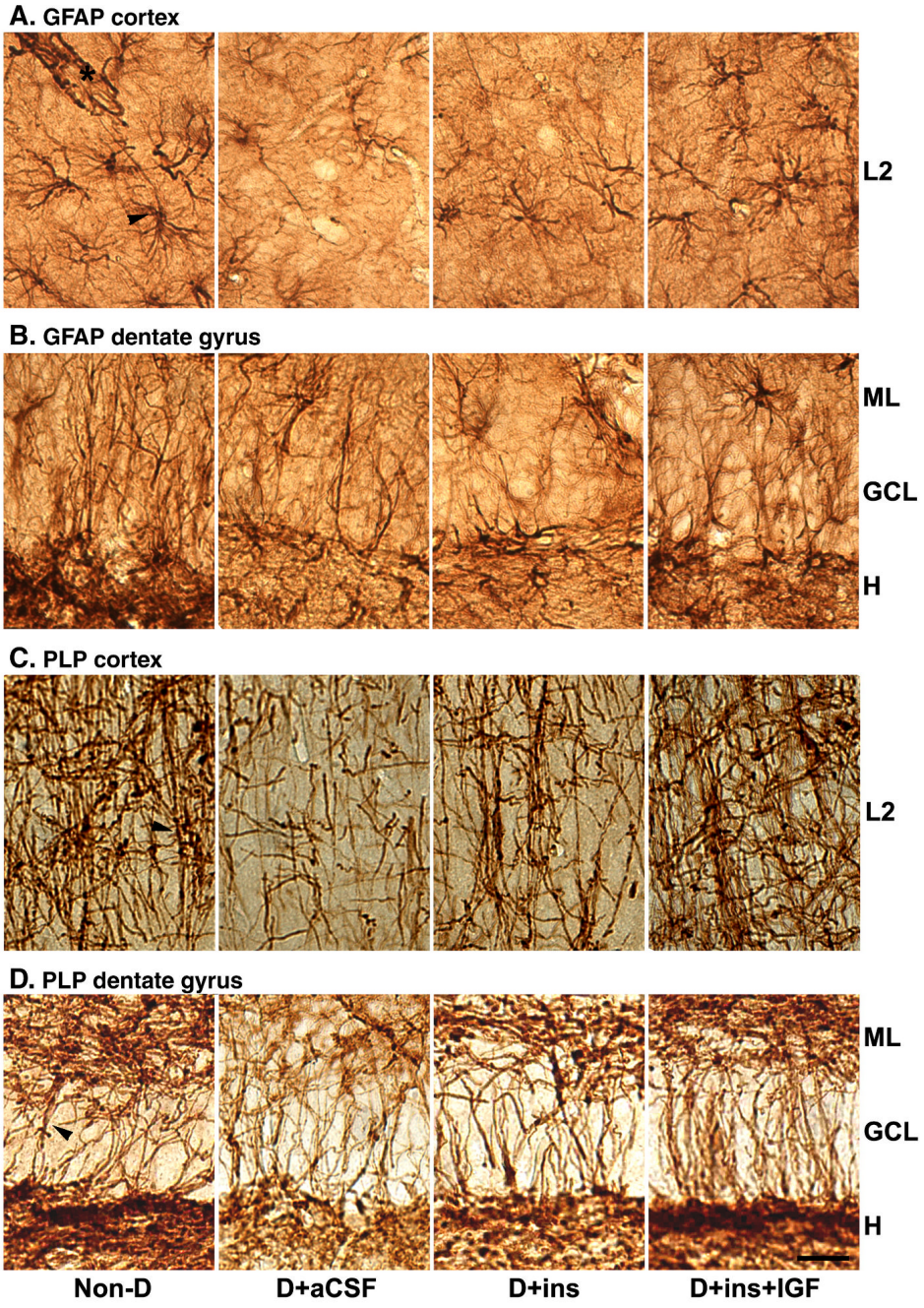

Fig. 6.

The effect of diabetes, insulin, or its combination with IGF on the immunohistochemical staining of glial GFAP and PLP in brain tissue sections from the cerebral cortex and hippocampal formation. A separate group of rats was transcardially perfused with paraformaldehyde and Vibratome coronal tissue sections were prepared from the cingulate cortex (top panels) consisting primarily of layer II or outer granular layer (L2). Other sections were from the dentate gyrus (DG) or CA1 regions of the hippocampal formation (bottom panels). The same primary antibodies used for Western blots were used for IHC. An avidin-biotin procedure and DAB was used for visualization. **A.** GFAP Cortex. The arrow head points to a star-shaped astrocyte, and the asterisk labels astrocytic end-feet on blood vessel in cortex.

B. GFAP DG. The DG region shows the molecular layer (ML), granule cell layer (GCL) and hilus (H). **C.** PLP cortex. Arrowhead points to PLP immunostaining of myelin associated with axons in cortex. **D.** PLP DG. Molecular layer (ML), granule cell layer (GCL) and hilus (H). Bar = 40 μm.

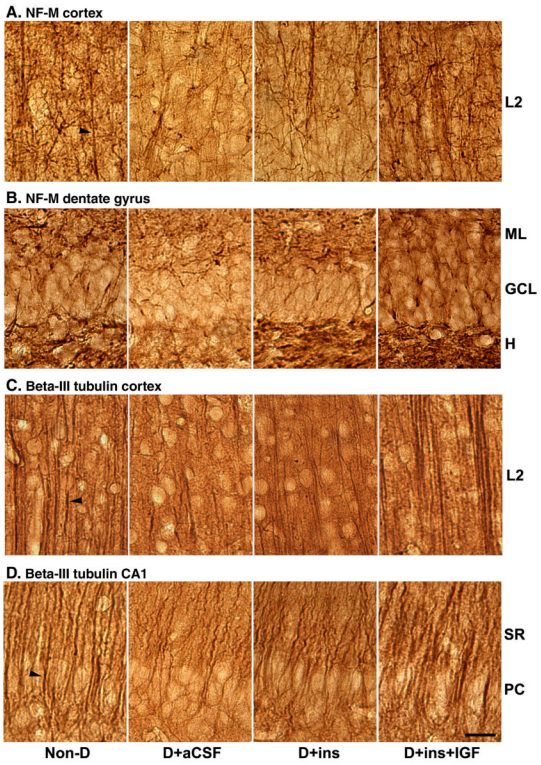

Fig. 7.

The effect of diabetes, insulin, or its combination with IGF on the immunohistochemical staining of neuronal β-tubulin class III and NF-M in brain tissue sections from cerebral cortex and hippocampal formation. Brain regions and labeling are as described in Fig. 6, except CA1 field of hippocampus is shown. **A**. NF-M Cortex. Arrowhead points to axons. **B.** NF-M DG. **C.** β-Tubulin class III Cortex. Arrowhead points to apical dendrite in cortex. **D.** β-Tubulin class III CA1. Arrowhead points to neurite in striatum radiatum (SR). Pyramidal cell layer, PC.

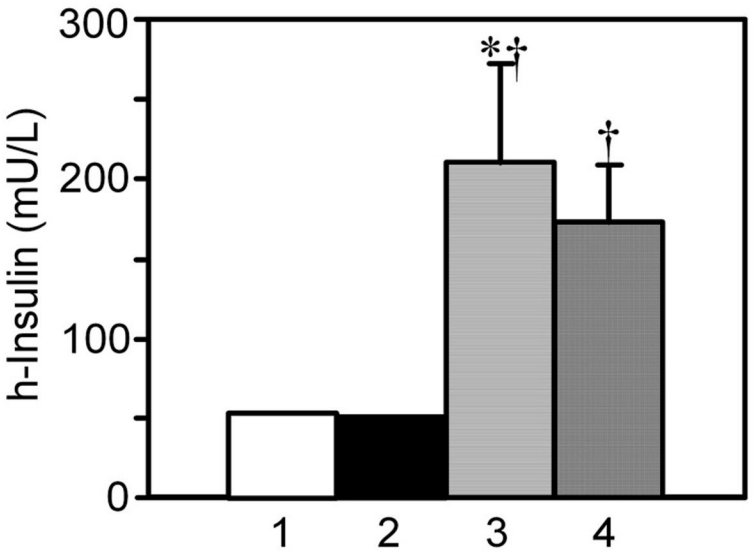

Fig. 8.

CSF insulin levels in diabetic rats infused *i.c.v.* with insulin or the combination treatment. At the conclusion of the experiment, CSF was withdrawn with a needle through the atlanto-occipital membrane at the cisterna magna. CSF was not successfully withdrawn from all animals, and rats from the brain biochemistry and perfusion studies were both used. The CSF was diluted 1:40 and insulin levels were measured by sandwich ELISA. Lane 1, (Non-D, N = 8); Lane 2, (D+aCSF, N = 12); Lane 3, (D+Ins, N = 9); and Lane 4, (D+Ins+IGF, N = 12). Error bars in Lanes 1 and 2 were too small to be shown.

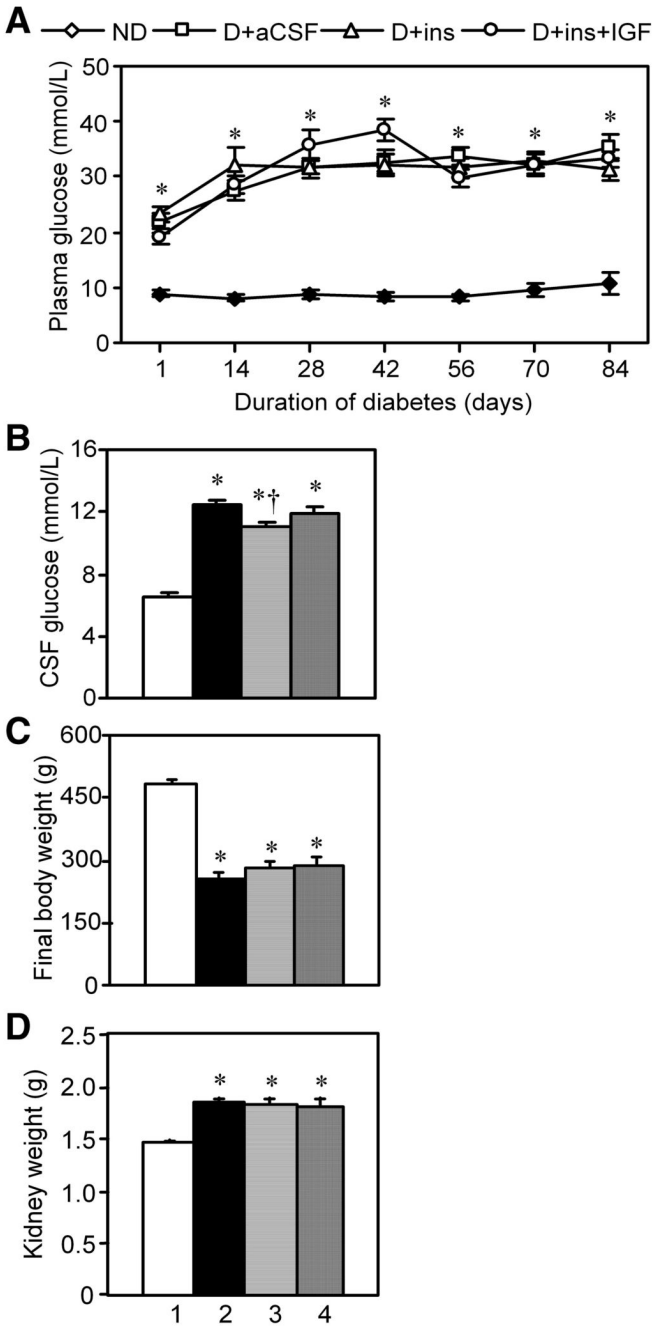

Fig. 9.

The effect of diabetes, insulin and its combination with IGF on plasma glucose levels, CSF glucose levels, rat body weights, and kidney weights. Lane 1, Non-D; Lane 2, D+aCSF; Lane 3, D+Ins; and Lane 4, D+Ins+IGF. Values are group means ± s.e.m. **A.** Plasma glucose levels at 2 week intervals. **B.** Final CSF glucose levels. **C.** Final rat body weights. **D.** Final kidney wet weights. Both kidneys were weighed.

Table 1

Summary of statistical comparisons

Parameter	D+aCSF vs. ND[a]	D+aCSF vs. D+ins vs. D+ins+IGF[b]	D+ins+IGF vs. D+ins[c]	ND vs. D+ins vs. D+ins+IGF[d]
Brain wet wt.	<0.013*	<0.025†	<0.018‡	<0.98
		<0.001†		<0.052
Brain dry wt.	<0.045*	<0.023†	<0.003‡	<0.99
		<0.001†		<0.002*
Brain water wt.	<0.010*	<0.030†	<0.037‡	<0.95
		<0.001†		<0.14
DNA	<0.029*	<0.78	<0.001‡	<0.20
		<0.001†		<0.001*
Total protein	<0.050*	<0.078	<0.61	<0.99
		<0.004†		<0.79
Actin	<0.003*	<0.850	<0.38	<0.021*
		<0.093		<0.44
α-tubulin	<0.001*	<0.49	<0.061	<0.009*
		<0.002†		<0.82
β-tubulin	<0.001*	<0.76	<0.15	<0.016*
		<0.017†		<0.71
GFAP	<0.001*	<0.008†	<0.024‡	<0.001*
		<0.001†		<0.15
GS	<0.14	<0.001†	<0.73	<0.20
		<0.011†		<0.70
PLP	<0.040*	<0.044†	<0.030‡	1
		<0.001†		<0.032*
MBP	<0.001*	<0.011†	<0.63	<0.64
		<0.001†		1
β-III tubulin	<0.001*	<0.24	<0.17	<0.003*
		<0.002†		<0.32
NF-L	<0.001*	<0.23	<0.18	<0.006*
		<0.002†		<0.42
NF-M	<0.001*	<0.80	<0.006‡	<0.001*
		<0.001†		<0.28

[a] Shows whether the parameter was significantly reduced in diabetes.

[b] Shows the effect of insulin alone or insulin's combination with IGF-I on the parameter in diabetes.

[c] Shows whether insulin's combination with IGF-I was more effective than insulin alone. Notice that combo treatment exceeded ND group in few cases.

[d] Shows whether the treatments normalized the parameter reduced in diabetes such that it no longer statistically differed from the non-diabetic group.

Significance accepted at $p<0.05$, Tukey-Kramer posthoc test of means.